Limnol. Oceanogr., 54(6), 2009, 1829–1844

The cold-water coral community as a hot spot for carbon cycling on continental margins: A food-web analysis from Rockall Bank (northeast Atlantic)

Dick van Oevelen,[a,*] Gerard Duineveld,[b] Marc Lavaleye,[b] Furu Mienis,[b] Karline Soetaert,[a] and Carlo H. R. Heip[a,b]

[a] Centre for Estuarine and Marine Ecology, Netherlands Institute of Ecology (NIOO-KNAW), Yerseke, The Netherlands
[b] Royal Netherlands Institute for Sea Research, Den Burg, The Netherlands

Abstract

We present a quantitative food-web analysis of the cold-water coral community, i.e., the assembly of living corals, dead coral branches and sediment beneath, associated with the reef-building *Lophelia pertusa* on the giant carbonate mounds at ~800-m depth at Rockall Bank. Carbon flows, 140 flows among 20 biotic and abiotic compartments, were reconstructed using linear inverse modeling by merging data on biomass, on-board respiration, $\delta^{15}N$ values, and literature constraints on assimilation and growth efficiencies. The carbon flux to the coral community was 75.1 mmol C m^{-2} d^{-1} and was partitioned among (phyto)detritus (81%) and zooplankton (19%). Carbon ingestion by the living coral was only 9% of the carbon ingestion by the whole community and was portioned among (phyto)detritus (72%) and zooplankton (28%). Carbon cycling in the community was dominated by suspension- and filter-feeding macrofauna associated with dead coral branches. Sediment traps mounted on a bottom lander trapped 0.77 mmol C m^{-2} d^{-1} (annual average), which is almost two orders of magnitude lower than total carbon ingestion (75.1) and respiration (57.3 mmol C m^{-2} d^{-1}) by the coral community. This discrepancy is explained in two ways: the coral community intercepts organic matter that would otherwise not settle on the seafloor, and through their action as ecosystem engineers, the increased turbulence generated by the coral framework and organic-matter depletion in the boundary layer augment the influx to the coral community. A comparison of macrofaunal biomass and respiration data with soft sediments reveals that coral communities are hot spots of biomass and carbon cycling along continental margins.

Oceans and seas cover almost 75% of Earth's surface and are underlain with predominantly soft sediments. In recent decades, however, increased use of underwater videos, video-guided sampling gear, and remotely operated vehicles (ROVs) has contributed to the discovery of other deep-sea ecosystems. One of the most spectacular examples are cold-water corals (CWCs). CWCs thrive in dark, cold, and mostly deep oceanic waters in several growth forms such as solitary colonies, coral patches, and complex reef structures or giant carbonate mounds that range in scale from meters to kilometers (Roberts et al. 2006). Dedicated mapping efforts in recent years have shown that CWCs occur in many parts of the world's oceans (Roberts et al. 2006), but they are specifically well developed along the continental slopes off Ireland, Rockall Bank, and on the Norwegian shelf. Unlike their tropical counterparts, CWCs lack symbiotic zooxanthellae and are independent of solar radiation. Instead, they live heterotrophically by filtering particles from the water column (Mortensen 2001).

The giant carbonate mounds in the SE Rockall Trough have well-developed CWC communities (van Weering et al. 2003; Mienis et al. 2009) that consist of a mosaic of living corals, dead coral branches and rubble, and sediment that is trapped in the coral framework (Freiwald et al. 2004). The top layer of a CWC community consists of coral branches that are covered by living coral tissue. Some species, such as the polychaete *Eunice norvegica*, live in symbiosis with the living coral (Roberts 2005), but, generally, the living coral zone is inhabited by few other species. Below or adjacent to the living coral layer in the coral community, there is a layer in which the coral has died. The dead branches form a substrate for a multitude of uni- and multicellular organisms that attach to the skeleton, such as bacteria, foraminifera, and smaller sessile epifauna like sponges, hydroids, and anemones (Freiwald et al. 2004; van Soest et al. 2007), or that live as mobile fauna at the surface or in hollows of the skeleton (e.g., Polychaeta and meiofauna; Raes and Vanreusel 2006). We refer to this assemblage of organisms as "biofilm" throughout this paper. Larger mobile epifauna, such as gastropods and sea urchins, also live on and in between the dead coral branches. In the sediment that accumulates between the coral branches, an infaunal benthic community develops. The assembly of living corals, dead coral branches, and trapped sediment forms the complex CWC ecosystem.

Ecological research on CWC communities has focused in particular on mapping and analysis of CWC occurrences in relation to seabed topography and environmental conditions in order to understand their distribution (Davies et al. 2008). These distribution maps have shown that CWCs thrive on topographic highs where hard substrate is available. These conditions allow for coral settlement while accelerated currents provide an advective flux of organic matter (OM). Model simulations with an idealized bottom topography indicate that CWC communities are typically found at places on the continental margin that have the highest particle encounter rates (Thiem et al. 2006). Coral presence at Porcupine Bank and Rockall Bank is dominat-

* Corresponding author: d.vanoevelen@nioo.knaw.nl

ed by the species *Lophelia pertusa* and seems to be directly linked to surface productivity, since downslope transport of surface waters provides a mechanism through which organic-rich surface water is transported to the coral community (White et al. 2005; Duineveld et al. 2007). Coral tissue analyzed for stable-isotope signatures (Duineveld et al. 2004, 2007; Kiriakoulakis et al. 2005) and fatty-acid composition (Kiriakoulakis et al. 2005) provides additional evidence that CWC growth largely depends on high-quality organic matter produced in the photic zone of the water column.

Quantitative research and process-oriented food-web research on CWC communities are hampered by their complex structure and limited accessibility. It has therefore been difficult to evaluate the importance of CWC ecosystems in terms of their ecosystem functioning and/or food-web structure. To date, no biomass records of CWC and associated fauna have been reported in the literature. Improved knowledge on the food web-structure, such as biomass, productivity, and trophic linkages, may also be valuable to substantiate calls for conservation of coral communities (Roberts et al. 2006). Here, we provide a first picture of carbon cycling in a complete CWC food web and compare measures of ecosystem functioning (i.e., biomass and carbon processing) with those of open-slope sediments.

Owing to their complex structure and difficult accessibility, data sets on CWC communities are archetypal examples of undersampled food webs. Vézina and Platt (1988) developed inverse modeling techniques to solve food-web models that suffer from data deficiency by merging the available quantitative data with a topological food-web model. In an inverse model, data on biomass and respiration are combined with literature data on assimilation and growth efficiencies. In a recent extension of the inverse methodology, van Oevelen et al. (2006) also integrated stable-isotope data in the food-web model and demonstrated that this improved the quality of the food-web reconstruction.

Here, we present the first comprehensive analysis of carbon cycling and food-web dynamics in a complete CWC community by integrating biomass, respiration, organic carbon burial, and $\delta^{15}N$ stable-isotope data using inverse modeling. The quantitative data were obtained by dedicated sampling of the CWC community on the giant carbonate mounds at Rockall Bank (NE Atlantic). The food-web structure reveals important carbon sources and transfer pathways in the food web. Ecosystem functioning, i.e., macrofaunal biomass stock and carbon processing, of the CWC community is gauged herein against that in benthic food webs along the continental margin.

Methods

Study site and cruises—The study site is located on the SE slope of Rockall Bank (Fig. 1A), where extensive carbonate mounds of several-hundred-meters height have been found between 600- and 1000-m water depth (van Weering et al. 2003; Mienis et al. 2007, 2009). The summits and upper flanks of these carbonate mounds are capped by living cold-water coral and a rich associated community, consisting of sponges, crinoids, and crustaceans (van Soest et al. 2007). For the present study, we focused on a large mound system at approximately 55°29.7′N, 15°48′E characterized by a rich coverage of live coral (Fig. 1B). The mound was visited with the RV *Pelagia* from the Royal Netherlands Institute for Sea Research (NIOZ) during several cruises in the summer months between 2001 and 2006.

Sampling and analytical procedures—Quantitative samples of living corals, associated organisms, and the underlying sediment were collected with a large (50-cm diameter) NIOZ-designed box corer. Some species that were too rare to be caught with a box corer, e.g., large decapods, amphipods, and fish, were collected with moored baited traps. Organisms were identified, counted, and their ash-free dry weight and carbon weights were estimated from wet weight using standard conversion factors. The ash-free dry weight of live corals and dead corals with epifauna was determined by drying at 60°C for 2 d and subsequent combustion at 500°C for 2 h.

Respiratory oxygen consumption of selected organisms from the box-core samples was measured while samples were contained in closed vials kept in a dark, temperature-controlled shipboard incubator. Since the number of incubation vials onboard was limited, respiration measurements were replicated only for those organisms for which it was estimated a priori that they would form an important fraction of the macrobenthic biomass. The temperature of the incubator was held at that of the bottom water using a Zephyr™ cooling machine. Incubation vials were equipped with a magnetic stirrer, a sensor for temperature, and an oxygen optode connected to FIBOX oxygen meters (Presens™) and a personal computer (PC). Vials were filled with bottom water collected using a conductivity–temperature–depth (CTD) rosette sampler. At the end of an incubation, a water sample was taken from the vial for oxygen measurement using Winkler titration. Incubations with bottom water were run parallel to correct for blank consumption. Sediment oxygen consumption was measured in acrylic cores taken from the box-core sample after overlying corals and fauna had been removed. The acrylic cores were closed with a stopper and a lid that contained a stirrer and an oxygen optode.

The methodology employed for measurement of nitrogen stable-isotope ratios ($\delta^{15}N$) in organisms is described in Duineveld et al. (2007). The stable-isotope ratio of a sample is expressed as per mil deviation (‰) from the isotope ratio of a reference material and is calculated as: $\delta^{15}N$ (‰) = $([R_{sample}]/[R_{atmN}] - 1) \times 1000$, in which R_{sample} is the $^{15}N:{}^{14}N$ ratio of the sample, and R_{atmN} is the $^{15}N:{}^{14}N$ ratio of atmospheric N_2 ($R_{atmN} = 0.0036765$).

Monthly mass and organic carbon fluxes to the study area were measured with a sediment trap (Technicap PPS4/3) mounted on the frame of a free-falling benthic Bottom Boundary (BOBO) lander with an aperture (0.05 m^2) at 4 m above the bottom. Each bottle of the sediment trap collected material for 30 d, and samples were preserved in a pH-buffered $HgCl_2$ solution in seawater. A detailed description of the lander configuration is given in Mienis

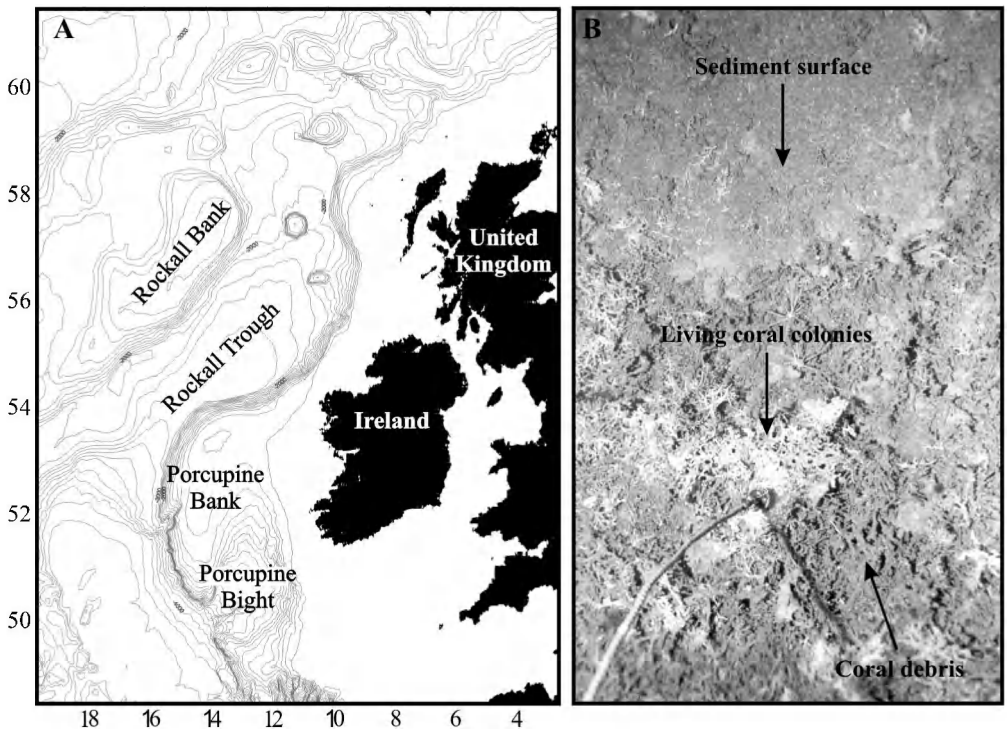

Fig. 1. (A) Location of the sampling site at Rockall Bank. (B) In situ picture of the CWC ecosystem with indicated living coral colonies, dead coral debris, and sediment surface. Note that the picture shows the three layers separated horizontally. In the samples that were used to determine biomass and respiration, however, these layers occurred in vertical alignment with living coral on top, dead coral structure in the middle, and underlying sediment.

et al. (2007). All samples were inspected with a stereomicroscope to remove swimmers when present and then were split and filtered on preweighed polycarbonate filters (47 mm, 0.47-μm pore size). Total organic carbon was analyzed with the Thermo Elemental Analyzer Flash EA 1112.

Food-web model—An inverse food-web model was developed to obtain a complete picture of the food-web structure in the coral community. In such a model, data on carbon cycling in the food web are cast in a matrix equation with equalities

$$\mathbf{A} \cdot \mathbf{x} = \mathbf{b} \tag{1}$$

and in one with inequalities

$$\mathbf{G} \cdot \mathbf{x} \geq \mathbf{h} \tag{2}$$

in which vector $\mathbf{x}$ contains the N individual food-web flows ($x_i, \ldots, x_N$). The equalities (Eq. 1) and inequalities (Eq. 2) provide quantitative information on the values of the food-web flows in $\mathbf{x}$. The equalities (Eq. 1) contain the mass balances of the different compartments and the data on process rates (e.g., respiration rates; *see* Food-web flows section), which are all linear functions of the flows. Each row in matrix $\mathbf{A}$ is a mass balance or data point expressed as a linear combination of the food-web flows, where the corresponding rate of change of a compartment (for mass balances) or numerical value (for data equations) is given in vector $\mathbf{b}$. The inequalities (Eq. 2) are used to place upper and/or lower bounds on single flows or combinations of flows, and the absolute values of the bounds are given in vector $\mathbf{h}$ and the constraints coefficients, signifying whether and how much a flow contributes to the constraint, are given in matrix $\mathbf{G}$. Soetaert and van Oevelen (2009) provide a pedagogical introduction to inverse modeling with explanatory examples.

The quantitative data can be conveniently divided into different data types: mass balances, food-web flows, biomass, conversion efficiencies, and stable-isotope signatures. These will be discussed in turn accordingly. The mass balances are set up a priori by defining compartments and linking them with flows (i.e., the topological food-web model). Empirical data that were available for the CWC community at Rockall Bank were respiration rates (data type: food-web flows), organic carbon burial (data type: food-web flows), biomass (data type: biomass), and δ^{15}N values (data type: stable-isotope signatures) and were implemented as equalities. In addition, literature data on assimilation and net growth efficiencies (*see* Conversion efficiencies) were implemented as inequalities. *See* next paragraphs for details.

The complete model consists of 140 flows, 20 mass balances, 31 additional data equalities, and 223 inequalities. The model $\mathbf{A} \cdot \mathbf{x} = \mathbf{b}$ and $\mathbf{G} \cdot \mathbf{x} \geq \mathbf{h}$ is solved for vector $\mathbf{x}$ by means of a Monte-Carlo sampling method. This method is explained in detail in Van den Meersche et al. (2009) and Soetaert and van Oevelen (2009). In short, a set

Table 1. Quantitative data of the CWC food web at Rockall Bank. The $\delta^{15}N$ data are from Duineveld et al. (2007). *See* legend of Fig. 2 for abbreviations. FT, feeding type; SF, suspension feeder; DF, deposit feeder; O, omnivore; and P, predator. "Stock" is expressed in mmol C m^{-2}, and "Respiration" is given in mmol C m^{-2} d^{-1}. Variability is indicated as standard deviations when available (the number of replicates in parentheses). The symbol "−" indicates "not available," and an empty cell indicates that the cell is irrelevant.

Compartment or process	Abbr.	FT	Stock	Respiration	$\delta^{15}N$	Value
Cold-water corals (*Lophelia pertusa* and *Madrepora oculata*)	CWC	SF	1222.0	1.83 ± 1.10 (9)	8.7 ± 0.22 (4)	
Eunice norvegica (Polychaeta)	EUN	SF, DF	310.6	0.35 ± 0.16 (2)	11.3 ± 1.23 (2)	
Biofilm	BIO		23,826.4	13.7 ± 17.26 (8)	6.0	
Hesionidae (Polychaeta)	HES	SF, DF	40.5	0.10 ± 0.01 (2)	9.5 ± 0.63 (2)	
Echinoidea (urchins)	URC	O/P	37.5	0.20 (1)	12.9 ± 0.33 (2)	
Porifera (sponges)	SPO	SF	607.8	2.3 ± 2.3 (9)	9.1 ± 2.64 (2)	
Asteroidea (starfish)	STA	O, P	18.7	0.014 (1)	11.7 ± 1.61 (2)	
Brachyura (crabs)	CRA	O, P	3.2	0.013 (1)	10.5 ± 1.99 (4)	
Hydrozoa	HYD	SF	123.2	0.34 (1)	8.6 ± 0.33 (2)	
Crinoidea	CRI	SF	16.6	0.014 (1)	7.4 ± 0.11 (2)	
Lima marioni (Bivalvia)	LIM	SF	22.9	0.13 ± 0.03 (4)	7.8 ± 0.30 (2)	
Asperarca nodulosa (Bivalvia)	ASP	SF	109.2	0.20 ± 0.02 (2)	8.9 ± 0.24 (2)	
Polychaeta	POL	SF, DF	16.2	—	9.5 ± 0.63*	
Bivalvia	BIV	SF	47.6	—	7.6 ± 0.36 (4)	
Suspension feeders	SUS	SF	172.5	—	8.6 ± 1.14 (8)	
Omnivores + predators	OMN	O, P	13.9	—	8.7 ± 0.93 (6)	
Fish	FIS	O, P	—	—	11.5 ± 0.46 (2)	
Benthic infauna	INF	DF	390.7	—	—	
Suspended detritus	DET_W				4.5†	
Phytodetritus	PHY_W				4.0†	
Zooplankton	ZOO_W				8.0†	
Sedimentary detritus	DET_S		8243.9			
Respiration sediment community				33.2 ± 10.01 (7)		
Trophic fractionation (‰)						3.4
Fractionation in biofilm (‰)						1.0
Carbon burial (mmol C m^{-2} d^{-1})						0.186

* Value assumed to be similar to the polychaete Hesionidae.
† Assumed value, *see* Stable-isotope signatures section.

of 10,000 food-web structures, i.e., vector **x**, is sequentially sampled. Each vector **x** is different but consistent with the matrix Eqs. 1 and 2. The mean and standard deviation for each food-web flow are calculated from this set of sampled solutions and represent a best estimate (i.e., the mean) and its associated uncertainty (i.e., standard deviation). The complete model formulation and solution routines run in the software R (R Development Core Team 2009), in the R-package LIM (http://lib.stat.cmu.edu/R/CRAN/web/packages/LIM/index.html). The input file of the CWC food-web model is included in the R-package LIM.

Mass balances—In the food-web model, we explicitly consider compartments from the three layers of living coral, dead coral branches, and trapped sediment that form the CWC community (Fig. 1). The compartments were decided upon by balancing biological detail and data availability. Species or groups of species for which $\delta^{15}N$ isotope signatures, biomass, and onboard respiration measurements were available were considered separately (Table 1). For some groups of species, only $\delta^{15}N$ isotope signatures and/or biomass data were available, and these were more coarsely grouped based on feeding type or taxonomy (Table 1). The model also considers the biofilm on the coral branches, which includes the microbial biofilm and that part of the epifauna and encrusting organisms that could not be separated from their substrate. Finally, the sedimentary compartments are infauna, bacteria, and detritus. Suspended food sources available to the coral community are phytodetritus, detritus, and zooplankton. We distinguished between labile phytodetritus and less labile detritus under the assumption that the $\delta^{15}N$ value of phytodetritus is typically lower than that of detritus due to diagenetic alteration (*see* Stable-isotope signatures section).

Diet information of all compartments was not available, and we used literature reports on gut content analysis and their feeding type (Table 1) to define the feeding links. The compartments cold-water corals, sponges, hydrozoa, crinoids, the bivalves *Lima marioni* and *Asperarca nodulosa*, and other suspension feeders were considered to feed solely on suspended food sources. The polychaete *Eunice norvegica* has been observed to steal food particles from coral polyps and to feed on administered food particles in the water column (Mortensen 2001; Roberts 2005). It was therefore assumed that they feed directly on suspended sources. Little is known about the feeding modes and preferences of Hesionidae (Polychaeta); they have been found to ingest algae, detritus, and a variety of prey items, including crustaceans, polychaetes, and sediment debris (Fauchald and Jumars 1979), possibly facilitated by

pumping behavior (Shaffer 1979). Possible food sources are therefore the biofilm (*see* the broad definition in the introduction), polychaetes, and all suspended food sources. Polychaetes can have a large variety of feeding modes (Fauchald and Jumars 1979) and were assumed to consume all suspended sources and the biofilm. Similarly, the omnivores + predators compartment (shrimps and gastropods) has feeding links with all suspended food sources and the biofilm. Crabs have a highly diverse diet and therefore have feeding links with all suspended food sources (Wieczorek and Hooper 1995; Whitman et al. 2001), the preys hydrozoans, crinoids, sponges, Hesionidae, and other polychaetes, the bivalves including *Lima marioni* and *Asperarca nodulosa*, other suspension feeders, omnivores + predators (Wieczorek and Hooper 1995), and the biofilm. Sea urchins are generalist feeders and have feeding links with the biofilm, Hesionidae, other polychaetes, sponges, hydrozoa, suspension feeders, and omnivores + predators (McClintock 1994). Starfish also have a broad food spectrum, including suspension feeders (Emson and Young 1994), biofilm, Hesionidae, other polychaetes, sponges, bivalves including *Lima marioni Asperarca nodulosa*, omnivores + predators, and urchins (McClintock 1994). The fish compartment consisted of rocklings (*Gaidropsarus* spp.) and codlings (*Moridae* sp.), which feed on suspended zooplankton, Hesionidae, other polychaetes, bryozoa (suspension feeders), and omnivores + predators (Houston and Haedrich 1986; Tully and Ceidigh 1989). The sedimentary food web is simple because of limited taxonomic resolution in the data. Sedimentary detritus is supplied from the water column and consumed by sedimentary bacteria and infauna. In turn, sedimentary bacteria are consumed by infauna.

Losses from the food web (e.g., migration or grazing by organisms not considered in the model) were combined into an export flow, which can be regarded as secondary production. Also, nonfeeding flows were considered: each biotic compartment respires carbon to dissolved inorganic carbon and produces feces to sedimentary or suspended detritus.

The (non-)feeding links in the food web define the mass balance for each compartment as $dC_i/dt = \Sigma\, x_{j\to i} - \Sigma\, x_{i\to k}$. The time derivatives are collected in $\mathbf{b}_{1\ldots M} = [dC_1/dt, \ldots, dC_M/dt]^T$. Biomasses were sampled once, and, without information on their temporal evolution, we assumed steady state: $\mathbf{b}_{1\ldots M} = 0$.

Food-web flows—Respiration rates were available for several compartments (Table 1), which can be directly appended as equalities (Soetaert and van Oevelen 2009).

Organic carbon burial was calculated from the sediment accumulation rate and organic carbon content at depth. Sediment accumulation was determined from ^{14}C dating of foraminifera shells and U/Th dating of cold-water corals collected in piston cores as 3.7 10^{-5} cm d^{-1} (De Haas et al. 2008). Sedimentary organic carbon content decreased exponentially with depth and was fitted with the function $C_x = C_{x0} \times e^{-kx} + C_\infty$ to derive the organic carbon content at "infinite" depth (C_∞ = 5030 mmol C m^{-2} cm^{-1}). The resulting organic carbon burial of 0.19 mmol C m^{-2} d^{-1} (Table 1) was included in Eq. 1.

Biomass—Lower and upper boundaries on respiration rates for compartments for which only biomass was available were estimated using an allometric scaling relation for deep-sea organisms (Mahaut et al. 1995). The respiration rate (R) of a compartment was calculated by multiplying its biomass with a biomass-specific respiration rate ($r = 0.0074W^{-0.24}$, d^{-1}). The lower boundary was defined as $R/2$, and the upper boundary was defined as $R \times 2$ to account for the uncertainty in this estimate. These boundaries are included in Eq. 2.

Stable-isotope signatures—The $\delta^{15}N$ isotope value of an organism j ($\delta^{15}N_j$) is a function of the relative contribution of its food sources i ($\alpha_{i\to j}$) when corrected for trophic fractionation (Δ): $\delta^{15}N_j = \Sigma\, \alpha_{i\to j} \cdot (\delta^{15}N_i + \Delta)$, with $\Sigma\, \alpha_{i\to j} = 1$. The relative diet contribution can be rewritten as function of the food-web flows ($x_{i\to j}$), i.e., $\alpha_{i\to j} = x_{i\to j}/\Sigma_i x_{i\to j}$, and can therefore be directly appended to Eq. 1 (van Oevelen et al. 2006). Trophic fractionation of ^{15}N was assumed to be the standard value of 3.4‰ (Minagawa and Wada 1984; Post 2002). The isotope data do not uniquely define the diet and trophic position of each compartment because of the many food sources of a compartment, but they do ensure that the diet of each consumer in the reconstructed food-web model is consistent with the isotope measurements (van Oevelen et al. 2006).

Stable-isotope data were available for almost all food-web compartments and for suspended detritus (Duineveld et al. 2007; *see* Table 1). The $\delta^{15}N$ value of suspended detritus of 4.5 is similar to values reported by Kiriakoulakis et al. (2005) for suspended material sampled close to the sediment floor with large-volume stand-alone pumping systems (SAPS, Challenger Oceanic) (range 4.2–7.3‰, average 5.2‰). The $\delta^{15}N$ value of suspended detritus is typically higher than that of phytodetritus, because detritus is a mixture of algal and zooplankton (heavier $\delta^{15}N$) derived OM, and diagenetic alteration generally leaves residual OM enriched in ^{15}N (Altabet 1996). Moreover, the lightest $\delta^{15}N$ value for macrofauna is 7.4‰ (Table 1), and, if we take trophic fractionation into account, this indicates that the lightest resource should be ≤4‰. We assumed 4‰ for phytodetritus, because it is also consistent with literature values for phytoplankton in the North Atlantic (Voss et al. 1996; Mienis et al. 2009). The nutrient status of surface waters can influence the $\delta^{15}N$ of phytoplankton, where typically low $\delta^{15}N$ values occur under nutrient-replete conditions, and elevated $\delta^{15}N$ values occur in nutrient-depleted conditions (Altabet 1996). However, $\delta^{15}N$ values of suspended matter collected with sediment traps are fairly constant and generally lie between 3‰ and 4‰ during periods of high primary production (Mienis et al. 2009). We therefore assumed a constant $\delta^{15}N$ value for phytodetritus and suspended detritus. Typical values for zooplankton $\delta^{15}N$ in temperate and northern seawater vary between 7‰ and 9‰ (Fry and Quinones 1994), and we assumed a $\delta^{15}N$ signature of 8‰. This value is also

consistent with +4‰ trophic fractionation with respect to phytodetritus (Wu et al. 1997).

A $\delta^{15}N$ value and trophic fractionation factor for the biofilm (consisting of bacterial and faunal biomass) was not available, and therefore the following procedure was followed. For the $\delta^{15}N$ biofilm value, we determined the range of $\delta^{15}N$ values that is consistent with the other data in the model and, as such, obtained a lower limit of 5.0‰ and upper limit of 6.8‰. The mean of this consistent range (5.9‰) was subsequently used as $\delta^{15}N$ of the biofilm on dead coral branches. The trophic fractionation factor of the biofilm was estimated based on the potential food sources for the biofilm: senescing CWC tissue (8.7‰), suspended phytodetritus (4‰), and detritus ($\delta^{15}N$ of 4.5‰). The fractionation factor of the biofilm should be a mix of bacterial and faunal trophic fractionation. Faunal trophic fractionation is ~3.4‰; information on fractionation during bacterial decay is limited, but it is lower than faunal fractionation and lies around 1‰ ± 0.4‰ (Altabet 1996). We tested the range of mixed fractionation factors (between 1‰ and 3.4‰) that was valid with the other data in the model. The resulting range of 1–1.7‰ was small, and we used the mean of 1.35‰ in the model. This low fractionation factor resembles closely the bacterial end member and indicates that bacteria are the biologically most active pool of nitrogen in the biofilm.

Conversion efficiencies—Finally, lower and upper bounds were placed on the assimilation efficiency and net growth efficiency. Respiration rates (R), either measured or determined from allometric scaling (*see* Biomass), were used to constrain the production rate (P) of a compartment using the net growth efficiency (NGE), which is the ratio $NGE = P/(P + R)$. The NGE is found to be independent of organism size, and the observed lower (30%) and upper (60%) boundaries for herbivores and carnivores (Calow 1977; Banse 1979; Hendriks 1999) were used for the faunal compartments. The growth efficiency of bacteria was constrained to 6–30%. This range encompasses growth efficiencies observed for growth on phytoplankton, phytodetritus, and feces (del Giorgio and Cole 1998). The assimilation efficiency (AE), i.e., the ratio of assimilation ($A = P + R$) to consumption (C), is independent of body size and lies between 40% and 80% for cold-blooded aquatic detritivores, herbivores, and carnivores (Banse 1979; Hendriks 1999). This range was used for all faunal compartments.

Sensitivity analysis—We acknowledge uncertainty in the aforementioned assumptions of a fixed trophic fractionation of 3.4‰ for every faunal compartment, the trophic fractionation of the biofilm, and the assumed isotope values for the biofilm and phytodetritus. To test the robustness of these assumptions we re-initialized the model 200 times with random parameter values and solved each successfully resampled model with the Monte-Carlo method as described previously for 250 times. The parameter values for trophic fractionation for each faunal compartment were sampled from a normal distribution with mean and standard deviation of 3.4‰ ± 0.98‰ (Post 2002); for trophic fractionation of the biofilm, they were sampled from a uniform distribution [1, 3.4]; and for the $\delta^{15}N$ biofilm, they were sampled from a uniform distribution [4 + fractionation biofilm, 8.7 + fractionation biofilm]. The mean and standard deviation for each flow in the set of 50,000 food-web structures (200 × 250) from the sensitivity analysis were compared with the results from the default model. The default solution has the values of the various parameters as in Table 1. The sensitivity analysis was based on random values for each parameter drawn from the ranges as discussed previously.

Results

Biomass and respiration-rate measurements—The total biomass in the CWC community was 26,980 mmol C m^{-2} (Table 1). The majority of organic carbon in the coral community was present in the biofilm on dead coral branches (23,826 mmol C m^{-2}). The remaining living biomass (3153 mmol C m^{-2}) was dominated by CWC (39%), sponges (19%), infauna (12%), *Eunice norvegica* (10%), suspension feeders (5%), hydrozoans (4%), and *Asperarca nodulosa* (3%). The other faunal compartments together constituted less than 2% of the living biomass. The fish compartments could be sampled only qualitatively for $\delta^{15}N$ analysis, and hence no fish biomass data were available.

Respiration by the sediment community was 33.2 mmol C m^{-2} d^{-1}, and respiration by the biofilm was 13.7 mmol C m^{-2} d^{-1} (Table 1). Faunal respiration, based on the onboard incubations, was highest for sponges (2.3 mmol C m^{-2} d^{-1}) and CWC (1.83 mmol C m^{-2} d^{-1}). Other compartments respired less than 0.35 mmol C m^{-2} d^{-1}, i.e., less than 1% of the summed measured respiration rates.

Food-web model output—The CWC food web is complex, and flow values returned by the model differed by orders of magnitude (Figs. 2, 3). The largest flow values are associated with carbon cycling by benthic bacteria and the biofilm (*see* definition in Introduction), which showed flows magnitudes in the order of tens of mmol C m^{-2} d^{-1} (Fig. 2A). Hence, the dominant carbon flows in the food web are mediated by microbes. Carbon flows relating to feeding and respiration by sponges, Bivalvia, suspension feeders, fish, and CWCs are also large, with values in the order of 1–5 mmol C m^{-2} d^{-1} (Fig. 2B). Flows that show up in Fig. 2B relate mostly to suspension feeders with a high biomass. The highest complexity in the food web is seen in the part of the food web that has flow values of <0.5 mmol C m^{-2} d^{-1} (Fig. 2C), which includes carbon flows that are associated with feeding and respiration of suspension feeders with lower biomass (e.g., hydrozoa, bivalves *Lima marioni* and *Asperarca nodulosa*). Some predation flows mediated by urchins also show up in this plot. Most of the predatory feeding links are, however, of even lower magnitude and show up only in Fig. 2D, where flows <0.05 mmol C m^{-2} d^{-1} are pictured. In addition, carbon flows associated with the suspension-feeding crinoids and *Lima marioni* and the predatory compartments crabs and starfish show up here.

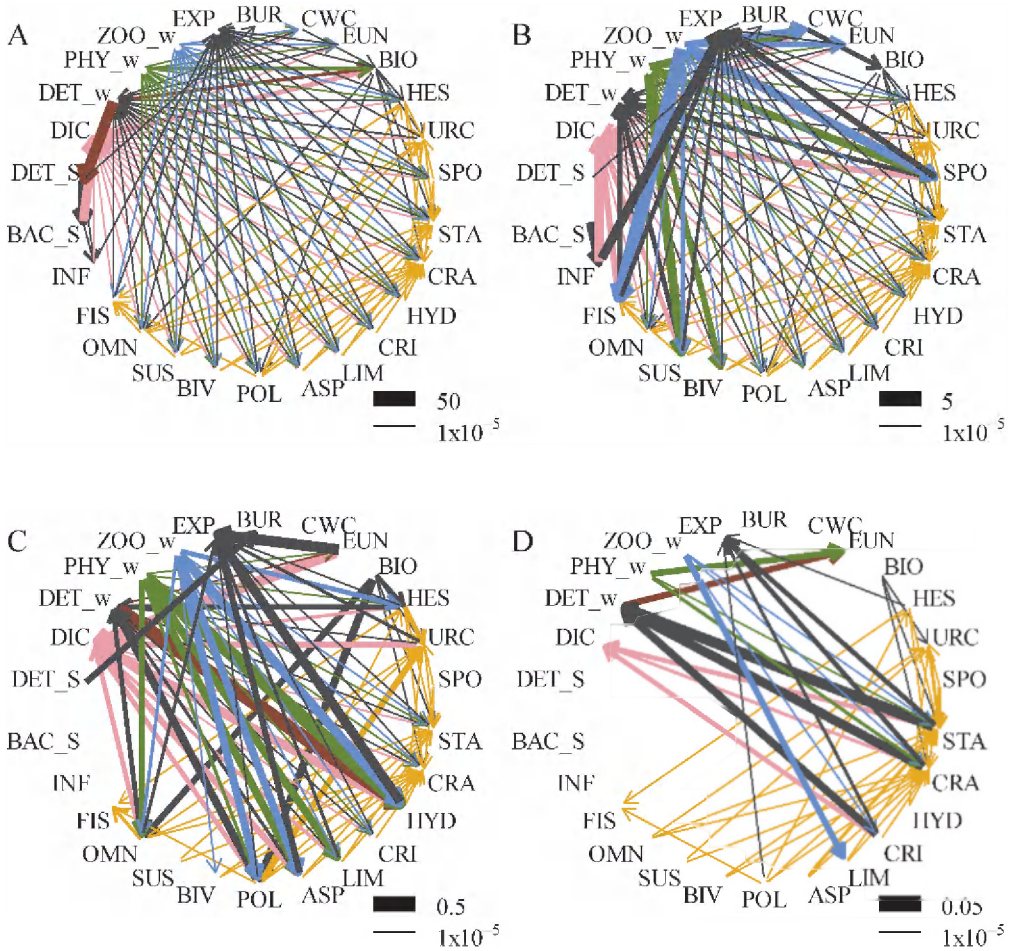

Fig. 2. Food-web flows returned by the food-web model, scaled to their magnitude, in the CWC food web at Rockall Bank (A–D). Because of the large differences in flow values, the results are plotted in four panels. All flows are only plotted in panel A. The plotted flows in panels B–D are truncated at maxima of 5, 0.5, and 0.05 mmol C m^{-2} d^{-1}, respectively, and thereby provide also insight into the structuring of flows of lower magnitude. For clarity, most flows are color-coded: flows PHY_w→… are green, DET_w→… are brown, ZOO_w→… are blue, …→DIC are pink, all flows between faunal compartments are orange, and other flows are in dark gray. Abbreviations are: ASP = *Asperarca nodulosa*, BAC_s = sedimentary bacteria, BIO = biofilm (*see* definition in Introduction), BIV = Bivalvia, CRA = crabs (Brachyura), BUR = burial, CRI = Crinoidea, CWC = cold-water corals, DET_s = sedimentary detritus, DET_w = detritus in water column, DIC = dissolved inorganic carbon, EUN = *Eunice norvegica*, EXP = export from community, FIS = fish (Pisces), HES = Hesionidae, HYD = Hydrozoa, INF = sedimentary infauna, LIM = *Lima marioni*, OMN = omnivores + predators, PHY_w = phytodetritus in water column, POL = Polychaeta, SPO = sponge (Porifera), STA = starfish (Asteroidea), SUS = suspension feeders, URC = urchins (Echinoidea), ZOO_w = zooplankton in water column.

The standard deviation of the flows indicates how well the flow is constrained by the data set. Overall, standard deviations are comparatively small for most flows, indicating that the food web is well constrained (Fig. 3). This is also shown by the coefficient of variation (CoV, i.e., the standard deviation normalized to the mean), which is <0.50 for 51% of the flows and is <0.75 for 77% of the flows. Flows with a relatively large standard deviation are of lowest magnitude (Fig. 3), which relate predominantly to predatory flows (Fig. 2D). Hence, the imposed data on the food-web model consisting of quantitative data on biomass, respiration, and physiology successfully constrain total ingestion and respiration rates by the compartments. In addition, the $\delta^{15}N$ values allow us to distinguish between the different food sources from the water column. The diets of the predators are, however, so diverse that the imposed information was insufficient to constrain the small predatory flows. Additional information is thus needed to further constrain the low-magnitude carbon flows that make up the diets of the predatory compartments.

Total carbon ingestion by the whole CWC community was 75.1 mmol C m^{-2} d^{-1} and was partitioned among the suspended resources as 19% zooplankton, 30% phytodetritus, and 51% detritus (Table 2). Organic carbon inges-

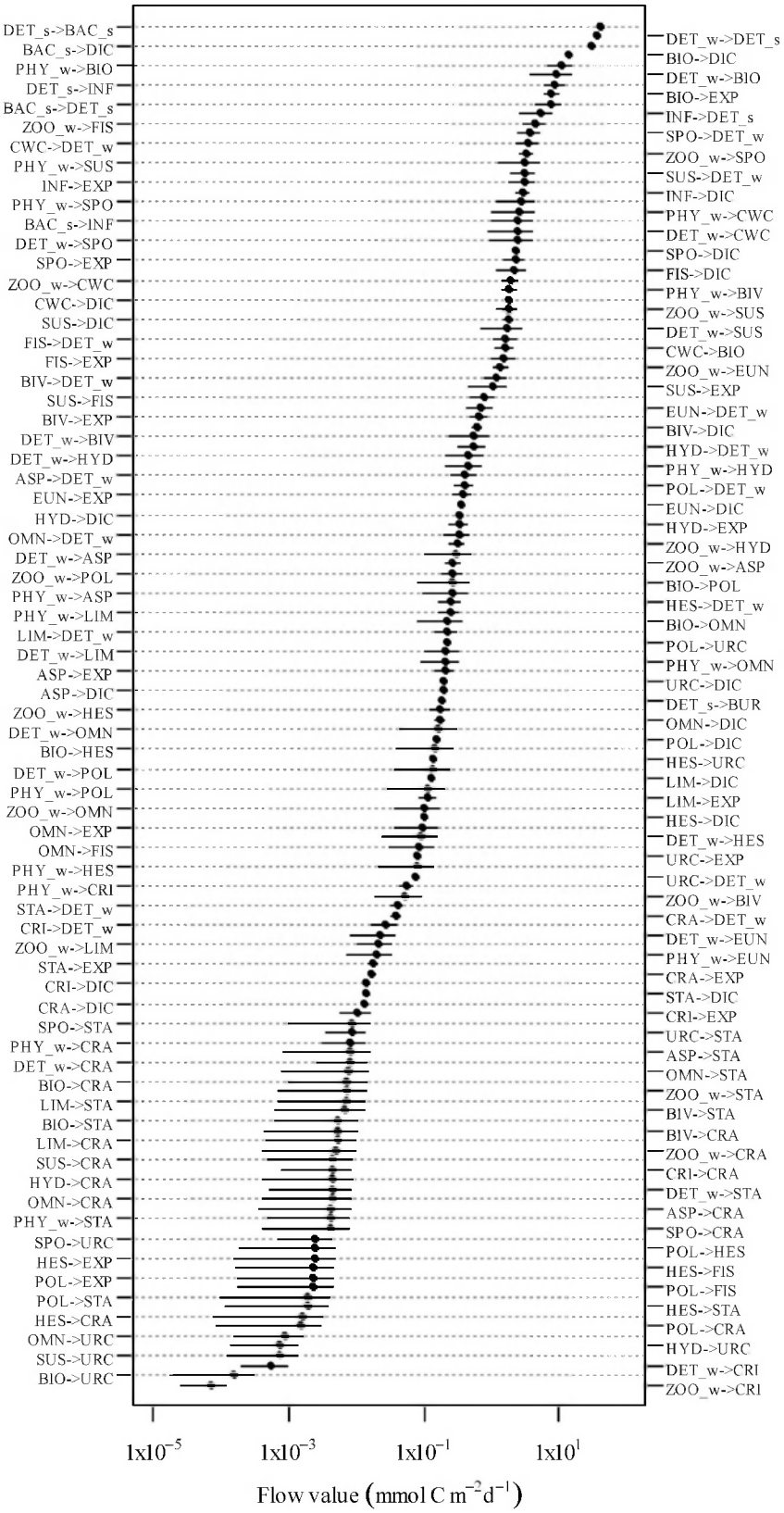

Fig. 3. Means and standard deviations of flow values in the CWC food web returned by the food-web model at Rockall Bank. *See* legend of Fig. 2 for abbreviations.

Table 2. Carbon sources of the CWC and the CWC community in mmol C m^{-2} d^{-1}.

	Zooplankton	Phytodetritus	Detritus
Living cold-water corals	1.97 (28%)	2.58 (37%)	2.46 (35%)
Coral community	14.1 (19%)	22.8 (30%)	38.1 (51%)

tion by the living cold-water corals was 7.01 mmol C m^{-2} d^{-1} and was partitioned among the resources as 28% zooplankton, 37% phytodetritus, and 35% detritus (Table 2).

Respiration by the complete CWC community derived from the model output, thus also including respiration of compartments for which no direct respiration measurements were available, was 57.3 mmol C m^{-2} d^{-1}. The positive difference between total carbon ingestion and respiration (17.8 mmol C m^{-2} d^{-1}) was partitioned between export (99%) and burial (1%). Major contributions to carbon export were the biofilm (44%), infauna (17%), sponges (12%), fish (9%), and suspension feeders (6%).

Sensitivity analysis—To obtain 200 successful random re-initializations of the food-web model, 18,587 attempts were needed. Hence, only 1.1% of the random re-initializations was successful, while the other re-initializations resulted in a model with parameter values that were inconsistent with the other data in the model. This means that only parameter values within a narrow range give a solvable model, and this suggests that the inferred food-web flows are insensitive against the assumptions for the δ^{15}N biofilm and trophic fractionation by fauna and the biofilm.

We evaluated the set of successful re-initializations (in which each successful re-initialization was solved 250 times; *see* above) in terms of relative and absolute difference of the average flow value. The structure of the food web will only be altered if the relative value of a flow changes drastically. The average flow values calculated in the sensitivity analyses differed less than 100% from the default solution for 84% of the flows, indicating that their values only changed moderately under the large parameter ranges that were used in the sensitivity analysis. The average flow value from the sensitivity analysis differed for only 10 out of the 140 flows more than 100% from the average value of the default model solution (Fig. 4) (*see* Web Appendix 1: www.aslo.org/lo/toc/vol_54/issue_6/1829a.pdf for listing of default solution and sensitivity analysis). Since the relative changes of these flow values are comparatively small, these differences will not affect the overall structure of the food web, although the absolute difference can be as high as 3.96 mmol C m^{-2} d^{-1} (Fig. 4). The relative difference for 22 flows was more than 100%, and the relative difference for 10 flows was more than 1000%. The absolute differences in these groups were small, however (<0.31 mmol C m^{-2} d^{-1}) (Fig. 4). For 10 flows, the relative difference between the average flow value from the sensitivity analysis and the default solution was high (e.g., a factor of 636 difference for the flow BIOFILM→URCHINS; Fig. 4). These flows were mostly related to the diets of urchins and crinoids. These results were reflected in the inferred diets of the faunal compartments, which did not change drastically apart from those of urchins and crinoids (Fig. 5).

Discussion

Data quality and the food-web model—We provide a first quantitative carbon budget of a CWC community (SE Rockall Bank) based on the integration of biomass, respiration, and stable-isotope data. We take an ecosystem approach to elucidate novel insights in the functioning of CWC food webs (Roberts et al. 2006). The quality of the food-web model depends, however, on the data quality and the assumptions in the model, and we therefore assess these critically.

Respiration rates of individual species and compartments were obtained from specimens sampled with a box core and brought into respiration chambers on the ship. Hence, specimens might experience responses due to decompression and removal from their habitat such that measured respiration rates may not reflect in situ values. The recovery depth of 800 m is much shallower than the generally accepted limit of 1500–2000 m (Rolff 2000), and thus direct decompression effects are expected to be small. Indeed, a comparison with measured biomass-specific respiration rates from the literature values shows that values from the CWC community are in the same order of magnitude (Fig. 6). The effects of removal from their natural habitat are, however, difficult to evaluate, since this is inevitable when obtaining species-specific respiration rates.

The biomass of the biofilm, i.e., the ash-free dry weight of the dead coral branches after all larger organisms were removed, was extremely high at 26,980 mmol C m^{-2} (Table 1). In this paper, we use the term biofilm in a broad sense including all unicellular and smaller multicellular organism living in and attached to the coral skeleton (*see* Introduction). Such a biofilm can trap suspended particles from the water column, and hence the biofilm biomass estimate represents a mixture of living and nonliving biomass (e.g., extracellular polymeric substances and particulate organic matter). This explains the low biomass-specific respiration of the biofilm (0.0006 d^{-1}) as compared to living organisms (Fig. 6). The organic carbon estimate for the biofilm is presented in Table 1 for reference, but it was not used in the model reconstruction of the food-web flows.

The δ^{15}N stable-isotope values provide important constraints on the trophic position and diet composition of organisms (Post 2002) and are typically evaluated by a mixing model. This mixing formulation can be straightforwardly implemented in the inverse model (*see* previous discussion) when one knows the δ^{15}N values of all

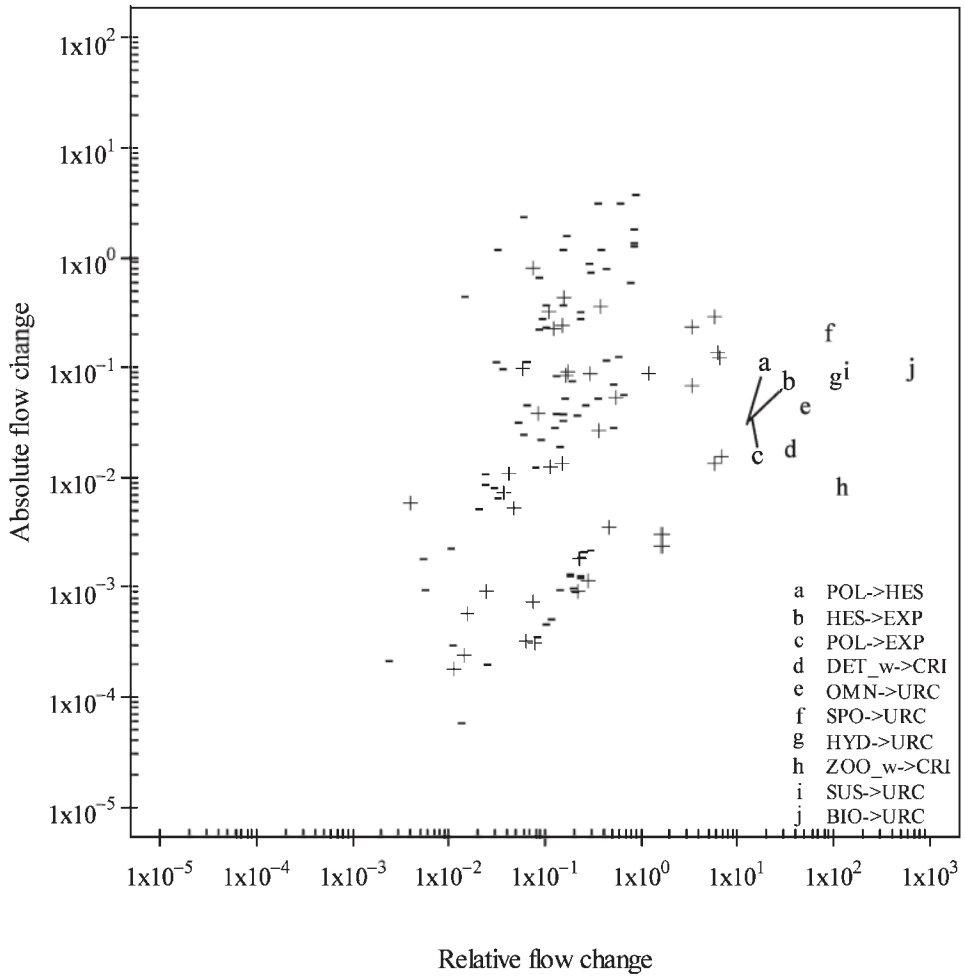

Fig. 4. Results from the uncertainty analysis of the food-web model plotted as relative difference (average flow value sensitivity analysis : average flow value default − 1) vs. absolute difference (average flow value sensitivity analysis − average flow value default). Positive differences are marked "+" and negative differences are marked as "−." The ten flows with largest relative differences, which are all positive differences, are indicated with lowercase letters. Letters a–c are offset with line segments to avoid overprinting.

compartments that may serve as food source, including the suspended food sources and the $\delta^{15}N$ trophic fractionation. Since it was impossible to assign specific $\delta^{15}N$ isotopic shifts for the individual flows, we adopted the commonly assumed isotope shift of 3.4‰ for all flows and included this parameter in the sensitivity analysis. Additional assumptions had to be made regarding the isotope values for the suspended food sources and trophic fractionation of the biofilm, but they could be resolved with other data constraints in the model and literature reports (*see* previous discussion). Moreover, the sensitivity analysis shows that the results of the default model are robust and insensitive against these assumptions (Figs. 4, 5).

Finally, the food-web model was solved under the assumption of steady state because data on biomass changes in time were not available. The CWC community resides at a depth of ~800 m in prevailing water temperatures between 7°C and 9°C (Duineveld et al. 2007). Against the large magnitudes of the flows, biomass increases are expected to be small, given the low temperature, and equating them to zero might not be too far from reality. Moreover, Vézina and Pahlow (2003) tested the commonly used assumption of steady state in numerical twin experiments under steady-state and non–steady-state conditions and concluded that the steady-state assumption had little influence on the accuracy of the reconstruction of ecosystem flows. Therefore, the steady-state assumption is unlikely to introduce large error in the food-web reconstruction.

Carbon cycling and food-web structure—To our knowledge, there is one earlier report on respiration of cold-water corals, though these were kept alive in aquaria, and it is therefore interesting to compare observations. Dodds et al. (2007) measured respiration under different temperature regimes and expressed their data on a per gram wet weight basis (including the carbonate skeleton). If we express our data in similar units, we arrive at a respiration rate of 0.069 μmol O_2 g^{-1} h^{-1}. This respiration rate is within, but at the lower end of, the values reported by Dodds et al.

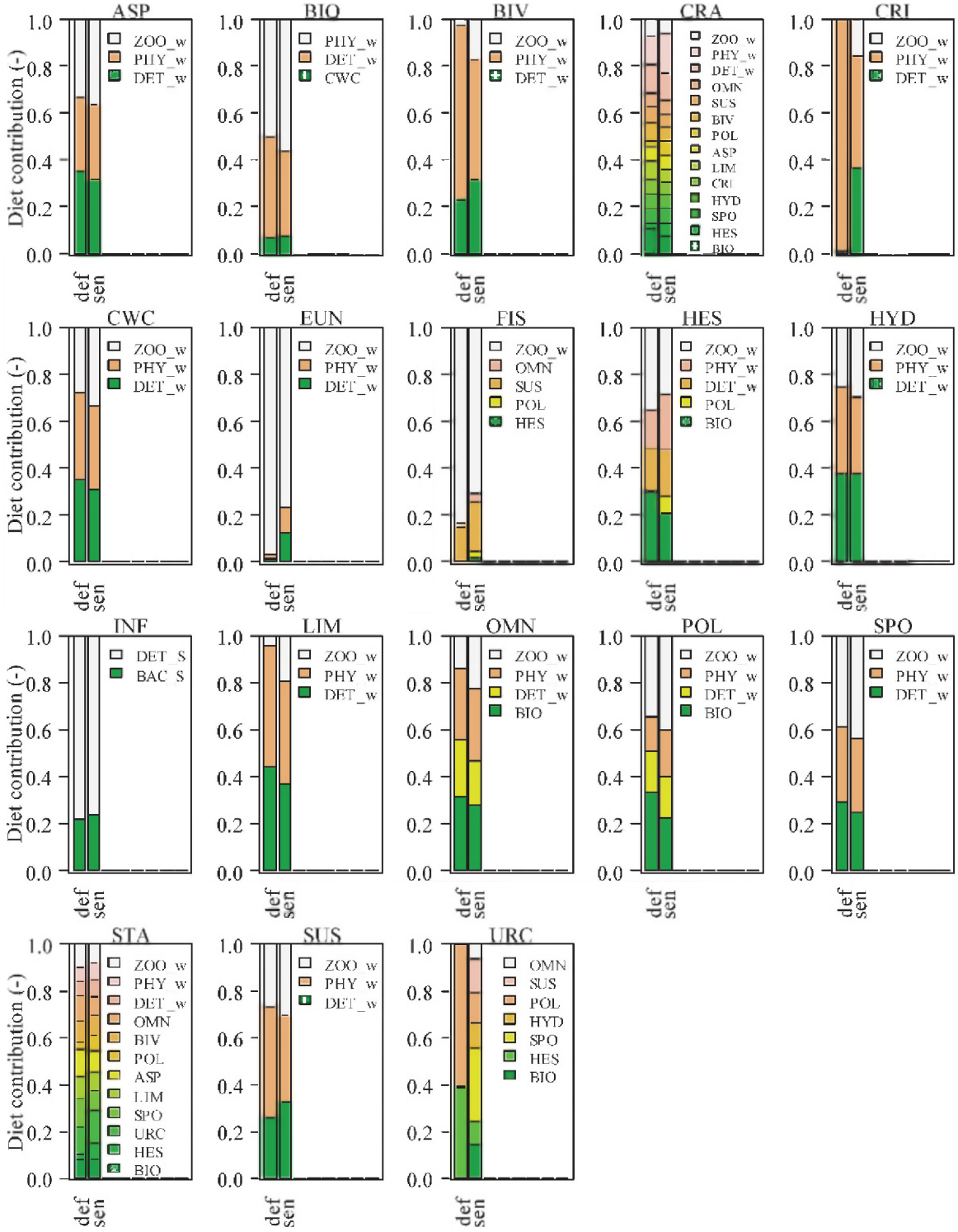

Fig. 5. Diet compositions of faunal compartments in the cold-water coral community in the default (def) solution and sensitivity (sen) analysis. *See* legend of Fig. 2 for abbreviations.

(2007). They used small pieces of coral branches (centimeters), which are likely to have a higher living biomass : skeleton ratio than the larger and thicker coral pieces (tenth of centimeters) used in this study. Hence, the biomass-specific respiration rates may be more similar than the previous calculation suggests.

There are several studies on possible food sources of CWCs. Laboratory observations include ingestion of living copepods and dead animal food particles (Mortensen 2001). Kiriakoulakis et al. (2005) found a comparatively high proportion of monounsaturated fatty acids (MUFAs) in the living tissue of CWCs, suggesting that zooplankton

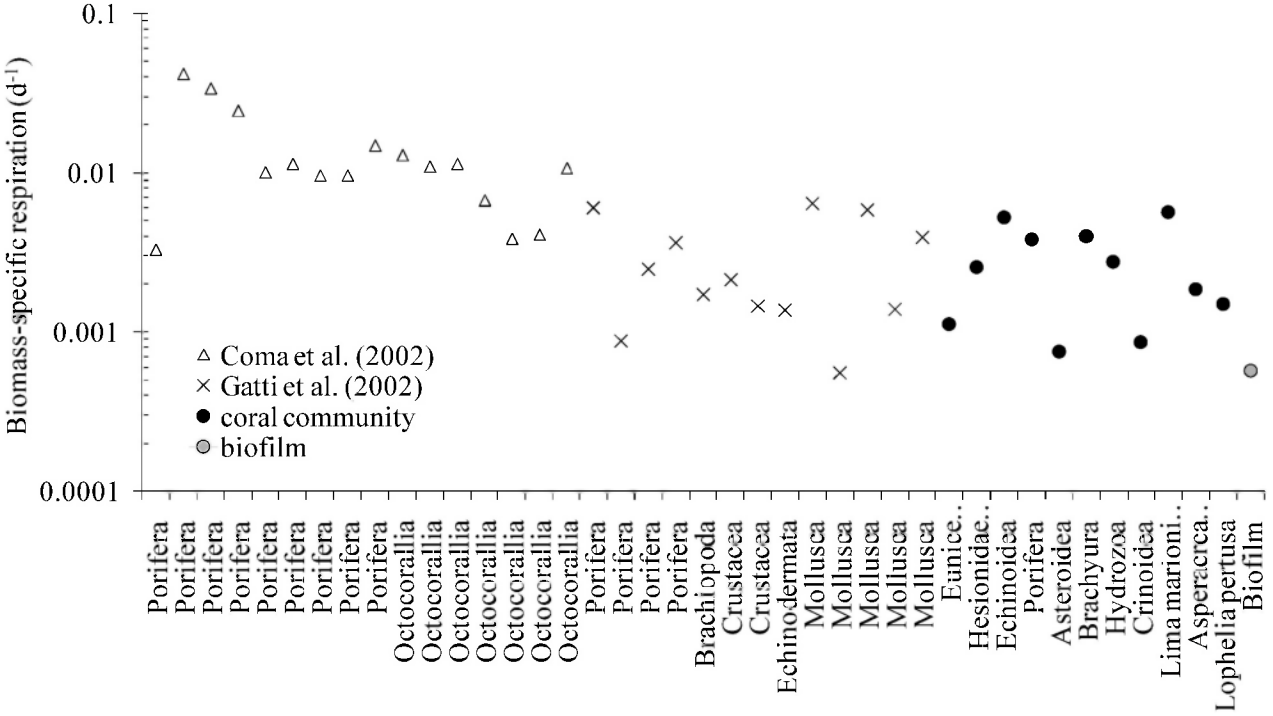

Fig. 6. Biomass-specific respiration rates (d^{-1}) from a literature overview of various temperate (Coma et al. 2002) and cold-water invertebrates (Gatti et al. 2002) against the measured respiration rates of the faunal compartments and the biofilm of the CWC community.

contribute to the diet of CWCs. Duineveld et al. (2004) concluded from $\delta^{13}C$ and $\delta^{15}N$ data that an algal–animal mix was the most likely diet of coral colonies on the Galicia Bank. Griffin and Druffel (1989) concluded from radiocarbon data of coral skeleton that surface-derived particulate organic carbon (POC) becomes part of the skeleton. The model results indicate that the CWCs at Rockall Bank derive most of their carbon from (phyto)detritus (72%) and only a small fraction from zooplankton (Table 2; Duineveld et al. 2007). Unfortunately, the isotope values of $\delta^{15}N$ for phytodetritus and detritus imposed on the model (Table 1) were not different enough to provide a good separation of these inputs to the food web (*see* Web Appendix 1).

The diet composition is mostly determined by the $\delta^{15}N$ stable-isotope values and may therefore be sensitive to the assumptions regarding the $\delta^{15}N$ signatures of the suspended resources. The most sensitive flows were related mostly to the diet composition of crinoids and urchins (Fig. 5), because in the default solution, their $\delta^{15}N$ could only be reproduced by a strong dominance of one food source (phytoplankton for crinoids, and polychaetes + Hesionidae for urchins). In the sensitivity analysis, however, the isotopic fractionation of $\delta^{15}N$ (fixed to 3.4‰ in the default solution) was relaxed, and a more balanced diet could also reproduce their diets (Fig. 5). Additional data on these diet compositions are needed to further constrain these flow values. Overall, however, the main structure of the food web is rather insensitive to the assumptions (Figs. 4, 5).

The model results show that the CWC and its associated community at Rockall Bank were primarily supported by detrital input. The large-scale bank topography at Porcupine Bank (Rockall Trough) causes upwelling of nutrient-rich waters that stimulates phytoplankton growth over the bank. A combination of different hydrodynamic processes causes rapid transport of freshly produced phytoplankton to the coral communities on the bank (White et al. 2005). Similarly, Davies et al. (2009) showed that the interaction between the reef complex and hydrography causes internal waves and advection of deep waters with high suspended matter, providing (phyto)detritus to the Mingulay reef complex (northeast Atlantic). CWC reefs on open shelfs, such as on the Norwegian continental shelf, may lack these large-scale processes that provide (phyto)detritus to the CWCs. Instead, these reefs are found teeming with zooplankton life, and the $\delta^{15}N$ values of CWCs are a several per mil heavier (indicative for a higher trophic position) than those from the NE Atlantic (Kiriakoulakis et al. 2005), suggesting that zooplankton may be more important. Since cold-water corals are able to exploit a variety of food sources (as observed in aquaria; Mortensen 2001), it may be large-scale processes that determine the availability of different food sources at a given location and thereby strongly influence the diet of the reef ecosystems at that location.

Sediment traps, mounted on bottom landers, were deployed for more than a year in the vicinity of the CWC community to estimate deposition of organic carbon

(Mienis et al. 2009). The average annual organic carbon deposition was 0.77 mmol C m^{-2} d^{-1} (monthly averages ranged from 0.24 to 1.44 mmol C m^{-2} d^{-1}) and was measured close to the sediment floor and therefore also includes resuspended OM (Mienis et al. 2009). Nevertheless, the OM deposition was almost two orders of magnitude lower than total carbon ingestion (75.1 mmol C m^{-2} d^{-1}) and respiration (57.3 mmol C m^{-2} d^{-1}) by the CWC community. There are two possible causes for this mismatch: either respiration rates do not reflect in situ values or the deposition rate estimated with sediment traps does not reflect organic carbon ingestion by the CWC community. We discussed the respiration rates previously and concluded that biomass-specific respiration rates compare favorably with literature records (Fig. 6). Inevitably, this implies that the flux measured with sediment traps undersamples the OM flux taken up by the coral community from the water column. Sediment traps may undersample depositional fluxes and may do so increasingly if the current speeds are high. Cylindrical traps suffer from limited undersampling at Reynolds numbers over the range 3000–43,000 (Gardner et al. 1997). This range in Reynolds numbers corresponds to a range in flow velocity of 2–27 cm s^{-1} for the type of sediment trap used. Current speeds measured on the lander ranged from 0 to 75 cm s^{-1}, daily averages ranged from 5 to 17 cm s^{-1}, and 30% of the records were >15 cm s^{-1} (Mienis et al. 2009). These currents speeds are in the upper regions, or in excess, of the range suggested by Gardner et al. (1997), such that undertrapping may be an issue. Sediment resuspension also increases with current speeds (Gardner et al. 1997), which leads to oversampling of the net sedimentation by bottom-mounted traps. Unfortunately, it is not possibly to quantify net sedimentation rates from the lander data (Mienis et al. 2009), but it is unlikely that the two-orders-of-magnitude difference between OM ingestion by the CWC community and OM trapping by the sediment traps is explained by undertrapping by the sediment traps.

A known example of the possible mismatch between carbon respiration by a soft-sediment community and carbon flux measured by sediment traps is reported by Smith et al. (2001). The authors inferred an organic carbon pulse about 20 times higher than that recorded by the sediment trap, which was moored close to the abyssal seafloor. Such large pulsing events were considered to be uncommon, and the mismatch was much lower during the complete 8-yr sampling period (Smith et al. 2001). The discrepancy found here for the CWC community is thus of a much larger magnitude than previously reported.

One explanation is that the CWC community acts as a biological filter that intercepts and traps OM from the water column that would otherwise not be deposited on the seafloor. Indeed, the biomass of filter feeders was 92% of total macrofaunal biomass, consistent with *Lophelia* banks on the Norwegian shelf (Jensen and Frederiksen 1992). These levels are unusually high as compared to other deep-sea and continental-slope food webs (Flach et al. 1998; Stora et al. 1999). In addition, the CWC community depletes the particle concentration in the lower layers of the benthic boundary layer, and its physical presence increases

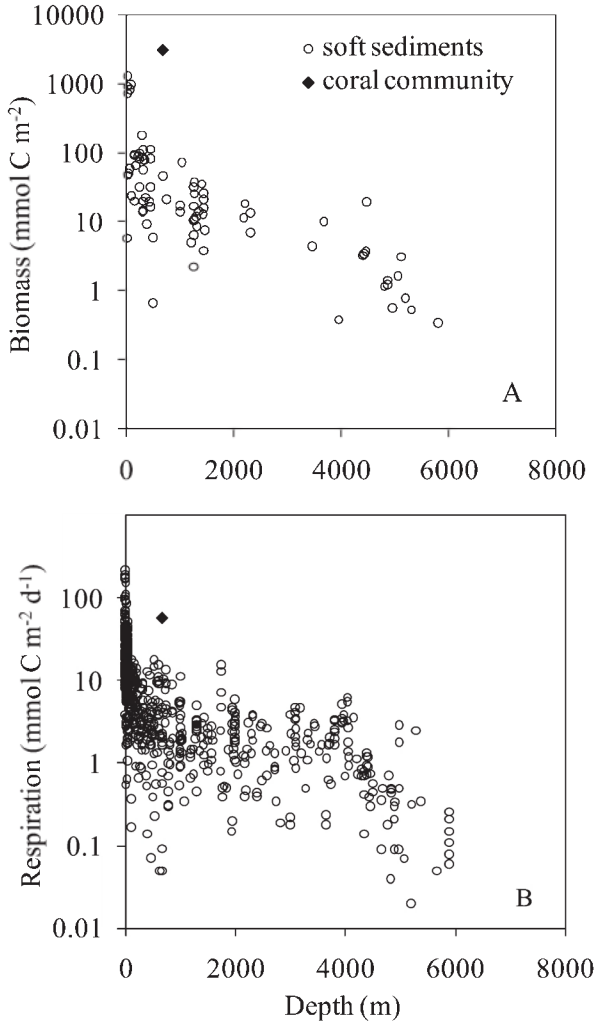

Fig. 7. (A) Macrobenthic biomass in soft-sediment food webs against water depth and in the CWC (summed macrobenthic biomass from Table 1). Biomass data from soft sediments are from Khripounoff et al. (1980), Sibuet et al. (1984), Richardson and Young (1987), Sibuet et al. (1989), Romero-Wetzel and Gerlach (1991), Rowe et al. (1991), Smith (1992), Rowe et al. (1997), Moodley et al. (1998), Albertelli et al. (1999), Heip et al. (2001), and Nodder et al. (2003). (B) Total respiration in soft sediment and the CWC food web, inferred from the food web model, against depth. Respiration rates from soft sediments are from Andersson et al. (2004).

turbulence levels. The combined effect may result in an increased particle flux towards the CWC. This is a classical example of ecosystem engineering, because the CWC structure modifies the particle flux by changing the physical environment. Ecosystem engineering is known for tropical coral reefs (Jones et al. 1994) and has been shown to elevate levels of ecosystem functioning, biomass, and biodiversity (Coleman and Williams 2002).

We evaluated ecosystem functioning and biomass by taking total respiration as a proxy for ecosystem functioning and macrobenthic biomass as biomass proxy. The natural choice of reference is soft-sediments on continental slopes and abyssal plains; these are well studied, but they lack the ecosystem engineering effect of CWC. Biomass and

ecosystem functioning in the CWC food web at Rockall are clearly enhanced as compared to soft sediments (Fig. 7). Macrobenthic biomass is almost two orders of magnitude higher in the CWC food web as compared to soft sediments at comparable water depth, and it is even higher than in shallow coastal sediments (Fig. 7A). Ecosystem functioning in the CWC community is also enhanced, though to a lesser extent, as compared to soft sediments at comparable depth (Fig. 7B). Hence, the engineering effect by the CWC is apparent at the level of the whole CWC ecosystem.

In addition, biodiversity appears to be higher in the CWC community than in surrounding soft sediments. Species richness of sponges in box-core samples of Rockall Bank with a dead coral cover of 10% or higher (26 species) is much higher than that of samples with a dead coral cover of less than 10% (two species) (van Soest et al. 2007). M. Lavaleye (unpubl. data) concluded from taxonomic analysis of the macrofauna of box-core samples with and without corals of Rockall Bank that total number of species per box core (94 vs. 33), the expected number of species $E_{S(80)}$ (28.2 vs. 24.7), and Shannon index (3.24 vs. 2.88) were higher in the CWC food web as compared to the adjacent sediments. Similar results were obtained by Henry and Roberts (2007), who found Shannon indexes of the coral-associated macrobenthos in the Belgica Mound Province and Porcupine Seabight to be significantly higher than surrounding sediments, while Jensen and Frederiksen (1992) found faunal diversity of CWC to rival that of tropical corals. We conclude that the CWC community at Rockall Bank is a hot spot of biomass, carbon cycling, and biodiversity. This conclusion is based on one CWC ecosystem, and it is presently unclear whether this holds true for other cold-water coral communities.

The OM flux toward the CWC community seems enhanced as compared to open-slope sediments (*see* comparison with sediment-trap data and slope sediments in Fig. 7B). The total export of OM from the surface ocean, however, cannot be enhanced, since the export of OM from the surface ocean depends on biological and physical processes in the euphotic zone. It may be that the enhanced OM flux is a result of local concentrating processes; i.e., the undirected export flux of OM is directed toward the CWC community by ecosystem engineering. This local concentration of OM flux may lower OM deposition away from the coral community, and an interesting question relates to the importance of this "redistribution" of OM flux and whether it influences the biology and biogeochemistry away from the reef.

Acknowledgments

The crew and technicians on board the RV *Pelagia* are thanked for their skilled work during sampling campaigns at Rockall. Two reviewers are thanked for their supportive and thoughtful comments that significantly improved the manuscript. This research was supported by the Hotspot Ecosystem Research on the Margins of the European Seas (HERMES) project (contract GOCE-CT-2005-511234), funded by the European Commission's Sixth Framework Programme under the priority "Sustainable Development, Global Change and Ecosystems." This is publication 4559 of the Netherlands Institute of Ecology (NIOO-KNAW), Yerseke.

References

Albertelli, G., A. Covazzi-Harriague, R. Danovaro, M. Fabiano, S. Fraschetti, and A. Pusceddu. 1999. Differential responses of bacteria, meiofauna and macrofauna in a shelf area (Ligurian Sea, NW Mediterranean): Role of food availability. J. Sea Res. **42:** 11–26.

Altabet, M. A. 1996. Nitrogen and carbon isotopic tracers of the source and transformation of particles in the deep sea, p. 155–184. *In* V. Ittekkot, P. Schäffer, S. Honjo, and P. J. Depetris [eds.], Particle flux in the ocean. Wiley.

Andersson, J. H., J. W. M. Wijsman, P. M. J. Herman, J. J. Middelburg, K. Soetaert, and C. Heip. 2004. Respiration patterns in the deep ocean. Geophys. Res. Lett. **31:** L03304, doi: 03310.01029/02003gl018756.

Banse, K. 1979. On weight dependence of net growth efficiency and specific respiration rates among field populations of invertebrates. Oecologia **38:** 111–126.

Calow, P. 1977. Conversion efficiencies in heterotrophic organisms. Biol. Rev. **52:** 385–409.

Coleman, F. C., and S. L. Williams. 2002. Overexploiting marine ecosystem engineers: Potential consequences for biodiversity. Trends Ecol. Evol. **17:** 40–44.

Coma, R., M. Ribes, J. M. Gili, and M. Zabala. 2002. Seasonality of in situ respiration rate in three temperate benthic suspension feeders. Limnol. Oceanogr. **47:** 324–331.

Davies, A. J., G. C. A. Duineveld, M. S. S. Lavaleye, M. J. N. Bergman, H. Van Haren, and J. M. Roberts. 2009. Downwelling and deep-water bottom currents as food supply mechanisms to the cold-water coral *Lophelia pertusa* (Scleractinia) at the Mingulay Reef complex. Limnol. Oceanogr. **54:** 620–629.

———, M. Wisshak, J. C. Orr, and J. M. Roberts. 2008. Predicting suitable habitat for the cold-water coral *Lophelia pertusa* (Scleractinia). Deep-Sea Res. I **55:** 1048–1062.

De Haas, H., F. Mienis, N. Frank, T. O. Richter, R. Steinacher, H. de Stigter, C. Van der Land, and T. C. E. Van Weering. 2008. Morphology and sedimentology of (clustered) cold-water coral mounds at the south Rockall Trough margins, NE Atlantic Ocean. Facies **55:** 1–26.

del Giorgio, P. A., and J. J. Cole. 1998. Bacterial growth efficiency in natural aquatic systems. Annu. Rev. Ecol. Syst. **29:** 503–541.

Dodds, L. A., J. M. Roberts, A. C. Taylor, and F. Marubini. 2007. Metabolic tolerance of the cold-water coral *Lophelia pertusa* (Scleractinia) to temperature and dissolved oxygen change. J. Exp. Mar. Biol. Ecol. **349:** 205–214.

Duineveld, G. C. A., M. S. S. Lavaleye, and E. M. Berghuis. 2004. Particle flux and food supply to a seamount cold-water coral community (Galicia Bank, NW Spain). Mar. Ecol. Prog. Ser. **277:** 13–23.

———, M. S. S. Lavaleye, M. I. N. Bergman, H. De Stigter, and F. Mienis. 2007. Trophic structure of a cold-water coral mound community (Rockall Bank, NE Atlantic) in relation to the near-bottom particle supply and current regime. Bull. Mar. Sci. **81:** 449–467.

Emson, R. H., and C. M. Young. 1994. Feeding mechanism of the brisingid starfish *Novodinia antillensis*. Mar. Biol. **118:** 433–442.

Fauchald, K., and P. A. Jumars. 1979. The diet of worms: A study of polychaete feeding guilds. Oceanogr. Mar. Biol. Ann. Rev. **39:** 193–284.

FLACH, E., M. LAVALEYE, H. DE STIGTER, AND L. THOMSEN. 1998. Feeding types of the benthic community and particle transport across the slope of the NW European continental margin (Goban Spur). Prog. Oceanogr. **42:** 209–231.

FREIWALD, A., J. H. FOSSÅ, A. GREHAN, T. KOSLOW, AND J. M. ROBERTS. 2004. Cold-water coral reefs. Out of sight—no longer out of mind. UNEP-WCMC Biodiversity Series 22. UNEP-WCMC. Cambridge, UK.

FRY, B., AND R. B. QUINONES. 1994. Biomass spectra and stable-isotope indicators of trophic level in zooplankton of the Northwest Atlantic. Mar. Ecol. Prog. Ser. **112:** 201–204.

GARDNER, W. D., P. E. BISCAYE, AND M. J. RICHARDSON. 1997. A sediment trap experiment in the Vema Channel to evaluate the effect of horizontal particle fluxes on measured vertical fluxes. J. Mar. Res. **55:** 995–1028.

GATTI, S., T. BREY, W. E. G. MULLER, O. HEILMAYER, AND G. HOLST. 2002. Oxygen microoptodes: A new tool for oxygen measurements in aquatic animal ecology. Mar. Biol. **140:** 1075–1085.

GRIFFIN, S., AND E. R. M. DRUFFEL. 1989. Sources of carbon to deep-sea corals. Radiocarbon **31:** 533–543.

HEIP, C. H. R., AND OTHERS. 2001. The role of the benthic biota in sedimentary metabolism and sediment-water exchange processes in the Goban Spur area (NE Atlantic). Deep-Sea Res. II **48:** 3223–3243.

HENDRIKS, A. J. 1999. Allometric scaling of rate, age and density parameters in ecological models. Oikos **86:** 293–310.

HENRY, L. A., AND J. M. ROBERTS. 2007. Biodiversity and ecological composition of macrobenthos on cold-water coral mounds and adjacent off-mound habitat in the bathyal Porcupine Seabight, NE Atlantic. Deep-Sea Res. I **54:** 654–672.

HOUSTON, K. A., AND R. L. HAEDRICH. 1986. Food-habits and intestinal parasites of deep demersal fishes from the upper continental-slope east of Newfoundland, Northwest Atlantic Ocean. Mar. Biol. **92:** 563–574.

JENSEN, A., AND R. FREDERIKSEN. 1992. The fauna associated with the bank-forming deep-water coral *Lophelia pertusa* (Scleractinaria) on the Faroe Shelf. Sarsia **77:** 53–69.

JONES, C. G., J. H. LAWTON, AND M. SHACHAK. 1994. Organisms as ecosystem engineers. Oikos **69:** 373–386.

KHRIPOUNOFF, A., D. DESBRUYERES, AND P. CHARDY. 1980. Benthic populations of the Vema fracture-zone—quantitative data and energy budget in the deep-sea environment. Ocean. Acta **3:** 187–198.

KIRIAKOULAKIS, K., E. FISHER, G. A. WOLFF, A. FREIWALD, A. GREHAN, AND J. M. ROBERTS. 2005. Lipids and nitrogen isotopes of two deep-water corals from the North-East Atlantic: Initial results and implication for their nutrition, p. 715–729. *In* A. Freiwald and J. M. Roberts [eds.], Cold-water corals and ecosystems. Springer-Verlag.

MAHAUT, M.-L., M. SIBUET, AND Y. SHIRAYAMA. 1995. Weight-dependent respiration rates in deep-sea organisms. Deep-Sea Res. I **42:** 1575–1582.

MCCLINTOCK, J. B. 1994. Trophic biology of Antarctic shallow-water echinoderms. Mar. Ecol. Prog. Ser. **111:** 191–202.

MIENIS, F., H. C. DE STIGTER, H. DE HAAS, AND T. C. E. VAN WEERING. 2009. Near-bed particle deposition and resuspension in a cold-water coral mound area at the Southwest Rockall Trough margin, NE Atlantic. Deep-Sea Res. I **56:** 1026–1038.

———, H. C. DE STIGTER, M. WHITE, G. DUINEVELD, H. DE HAAS, AND T. C. E. VAN WEERING. 2007. Hydrodynamic controls on cold-water coral growth and carbonate-mound development at the SW and SE Rockall Trough margin, NE Atlantic Ocean. Deep-Sea Res. I **54:** 1655–1674.

MINAGAWA, M., AND E. WADA. 1984. Stepwise enrichment of ^{15}N along food chains: Further evidence and the relation between $\delta^{15}N$ and animal age. Geochim. Cosmochim. Acta **48:** 1135–1140.

MOODLEY, L., C. H. R. HEIP, AND J. J. MIDDELBURG. 1998. Benthic activity in sediments of the northwestern Adriatic Sea: Sediment oxygen consumption, macro- and meiofauna dynamics. J. Sea Res. **40:** 263–280.

MORTENSEN, P. B. 2001. Aquarium observations on the deep-water coral *Lophelia pertusa* (L., 1758) (Scleractinia) and selected associated invertebrates. Ophelia **54:** 83–104.

NODDER, S. D., C. A. PILDITCH, P. KEITH PROBERT, AND J. A. HALL. 2003. Variability in benthic biomass and activity beneath the Subtropical Front, Chatman Rise, SW Pacific Ocean. Deep-Sea Res. I **50:** 959–985.

POST, D. M. 2002. Using stable isotopes to estimate trophic position: Models, methods, and assumptions. Ecology **83:** 703–718.

RAES, M., AND A. VANREUSEL. 2006. Microhabitat type determines the composition of nematode communities associated with sediment-clogged cold-water coral framework in the Porcupine Seabight (NE Atlantic). Deep-Sea Res. I **53:** 1880–1894.

R DEVELOPMENT CORE TEAM. 2009. R: A language and environment for statistical computing [Internet]. R Foundation for Statistical Computing. Available from http://www.R-project.org. Vienna.

RICHARDSON, M. D., AND D. K. YOUNG. 1987. Abyssal benthos of the Venezuela basin, Caribbean Sea—standing stock considerations. Deep-Sea Res. **34:** 145–164.

ROBERTS, J. M. 2005. Reef-aggregating behaviour by symbiotic eunicid polychaetes from cold-water corals: Do worms assemble reefs? J. Mar. Biol. Assoc. UK **85:** 813–819.

———, A. J. WHEELER, AND A. FREIWALD. 2006. Reefs of the deep: The biology and geology of cold-water coral ecosystems. Science **312:** 543–547.

ROLFF, C. 2000. Seasonal variation in delta C-13 and delta N-15 of size-fractionated plankton at a coastal station in the northern Baltic proper. Mar. Ecol. Prog. Ser. **203:** 47–65.

ROMERO-WETZEL, M. B., AND S. A. GERLACH. 1991. Abundance, biomass, size-distribution and bioturbation potential of deep-sea macrozoobenthos on the Voring Plateau (1200–1500-m, Norwegian Sea). Meeresforsch. Rep. Mar. Res **33:** 247–265.

ROWE, G. T., G. S. BOLAND, E. G. E. BRIONES, M. E. CRUZKAEGI, A. NEWTON, D. PIEPENBURG, I. WALSH, AND J. DEMING. 1997. Sediment community biomass and respiration in the Northeast Water Polynya, Greenland: A numerical simulation of benthic lander and spade core data. J. Mar. Syst. **10:** 497–515.

———, M. SIBUET, J. DEMING, A. KHRIPOUNOFF, J. TIETJEN, S. MACKO, AND R. THEROUX. 1991. Total sediment biomass and preliminary estimates of organic-carbon residence time in deep-sea benthos. Mar. Ecol. Prog. Ser. **79:** 99–114.

SHAFFER, P. L. 1979. Feeding biology of *Podarke pugettensis* (Polychaeta, Hesionidae). Biol. Bull. **156:** 343–355.

SIBUET, M., C. E. LAMBERT, R. CHESSELET, AND L. LAUBIER. 1989. Density of the major size groups of benthic fauna and trophic input in deep basins of the Atlantic Ocean. J. Mar. Res. **47:** 851–867.

———, C. MONNIOT, D. DESBRUYERES, A. DINET, A. KHRIPOUNOFF, G. ROWE, AND M. SEGONZAC. 1984. Benthic populations and trophic characteristics in the Demerare abyssal basin (Atlantic Ocean). Ocean. Acta **7:** 345–358.

SMITH, K. L. 1992. Benthic boundary layer communities and carbon cycling at abyssal depths in the central north Pacific. Limnol. Oceanogr. **37:** 1034–1056.

———, R. S. KAUFMANN, R. J. BALDWIN, AND A. F. CARLUCCI. 2001. Pelagic–benthic coupling in the abyssal eastern North Pacific: An 8-year time-series study of food supply and demand. Limnol. Oceanogr. **46:** 543–556.

SOETAERT, K., AND D. VAN OEVELEN. 2009. Modeling food web interactions in benthic deep-sea ecosystems: A practical guide. Oceanography **22:** 130–145.

STORA, G., M. BOURCIER, A. ARNOUX, M. GERINO, J. LE CAMPION, F. GILBERT, AND J. P. DURBEC. 1999. The deep-sea macrobenthos on the continental slope of the northwestern Mediterranean Sea: A quantitative approach. Deep-Sea Res. I **46:** 1339–1368.

THIEM, O., E. RAVAGNAN, J. H. FOSSA, AND J. BERNTSEN. 2006. Food supply mechanisms for cold-water corals along a continental shelf edge. J. Mar. Syst. **60:** 207–219.

TULLY, O., AND P. O. CEIDIGH. 1989. The ichthyoneuston of Galway Bay (west of Ireland). 2. Food of post-larval and juvenile neustonic and pseudoneustonic fish. Mar. Ecol. Prog. Ser. **51:** 301–310.

VAN DEN MEERSCHE, K., K. SOETAERT, AND D. VAN OEVELEN. 2009. xsample(): An R function for sampling linear inverse problems. J. Stat. Softw. **30:** 1–15.

VAN OEVELEN, D., K. SOETAERT, J. J. MIDDELBURG, P. M. J. HERMAN, L. MOODLEY, I. HAMELS, T. MOENS, AND C. H. R. HEIP. 2006. Carbon flows through a benthic food web: Integrating biomass, isotope and tracer data. J. Mar. Res. **64:** 1–30.

VAN SOEST, R. W. M., D. F. R. CLEARY, M. J. DE KLUIJVER, M. S. S. LAVALEYE, C. MAIER, AND F. C. VAN DUYL. 2007. Sponge diversity and community composition in Irish bathyal coral reefs. Contrib. Zool. **76:** 121–142.

VAN WEERING, T. C. E., H. DE HAAS, H. C. DE STIGTER, H. LYKKE-ANDERSEN, AND I. KOUVAEV. 2003. Structure and development of giant carbonate mounds at the SW and SE Rockall Trough margins, NE Atlantic Ocean. Mar. Geol. **198:** 67–81.

VÉZINA, A. F., AND M. PAHLOW. 2003. Reconstruction of ecosystem flows using inverse methods: How well do they work? J. Mar. Syst. **40:** 55–77.

———, AND T. PLATT. 1988. Food web dynamics in the ocean. I. Best-estimates of flow networks using inverse methods. Mar. Ecol. Prog. Ser. **42:** 269–287.

VOSS, M., M. A. ALTABET, AND B. VONBODUNGEN. 1996. delta N-15 in sedimenting particles as indicator of euphotic-zone processes. Deep-Sea Res. I **43:** 33–47.

WHITE, M., C. MOHN, H. DE STIGTER, AND G. MOTTRAM. 2005. Deep-water coral development as a function of hydrodynamics and surface productivity around the submarine banks of the Rockall Trough, NE Atlantic, p. 503–514. *In* A. Freiwald and J. M. Roberts [eds.], Cold-water corals and ecosystems. Springer-Verlag.

WHITMAN, K. L., J. J. MCDERMOTT, AND M. S. OEHRLEIN. 2001. Laboratory studies on suspension feeding in the hermit crab *Pagurus longicarpus* (Decapoda: Anomura: Paguridae). J. Crustac. Biol. **21:** 582–592.

WIECZOREK, S. K., AND R. G. HOOPER. 1995. Relationship between diet and food availability in the snow crab *Chionoecetes opilio* (O-Fabricius) in Bonne Bay, Newfoundland. J. Crustac. Biol. **15:** 236–247.

WU, J. P., S. E. CALVERT, AND C. S. WONG. 1997. Nitrogen isotope variations in the subarctic northeast Pacific: Relationships to nitrate utilization and trophic structure. Deep-Sea Res. I **44:** 287–314.

Associate editor: Anthony Larkum

Received: 11 November 2008
Accepted: 28 May 2009
Amended: 14 June 2009